

## LARGE AREA n-TYPE SILICON SOLAR CELLS WITH SELECTIVE FRONT SURFACE FIELD AND SCREEN PRINTED ALUMINUM-ALLOYED REAR EMITTER

F. Book, T. Wiedenmann, A. Dastgheib-Shirazi, B. Raabe, G. Hahn

University of Konstanz, Department of Physics, Jacob-Burckhardt-Str. 29, 78464 Konstanz, Germany  
Tel: +49-7531-88-2074, Fax: +49-7531-88-3895, Email: Felix.Book@uni-konstanz.de

**ABSTRACT:** Large area n-type silicon solar cells with a screen-printed aluminum rear side emitter are mainly limited by their front surface recombination velocity. In order to overcome this limitation, we use an industrially applicable etch-back process to create a selective front surface field (s-FSF). This process was developed for the formation of a single diffusion selective emitter on p-type silicon; it generates a deep doping profile with a low surface concentration which results in an excellent emitter saturation current and a highest independently confirmed stable cell efficiency of 18.7% on 5" p-type Cz silicon.

In this work we focus on the applicability of this process to n-type silicon. 6" solar cells with different front side etch-back depths have been processed from n-type silicon leading to a highest efficiency of 18.5% for a s-FSF cell and an average gain of 0.8%<sub>abs</sub> compared to cells with a homogeneous FSF. We furthermore investigate the quality of the etch-back FSF and the screen printed alloyed emitter from different pastes by QSSPC measurements.

Keywords: n-type, etching, selective emitter

### 1 INTRODUCTION

Although p-type silicon is the dominating base material for today's industrial-type solar cells, it poses a fundamental limitation to the cell efficiency due to the light-induced degradation of Cz silicon and the higher sensitivity to metal impurities [2, 3]. For high efficiency solar cells these effects can be avoided by using n-type silicon. If the standard screen-printing process is applied, this results in a solar cell with a rear aluminum emitter and a phosphorous front surface field [3, 4]. Since most of the charge carriers are generated close to the front surface but are collected at the rear emitter, a high bulk lifetime and low front surface recombination velocity (SRV) are crucial for this cell type. It is therefore necessary to use high ohmic base material and a low sheet resistance FSF. In order to obtain a low front contact resistance, advanced metallization techniques can be applied [5]. If Ag screen printing is used for front side metallization, a good contact resistance can be achieved by creating a selective FSF with a low sheet resistance in the contacted area [6, 7].

We have developed a simple and industrially applicable production sequence that uses one diffusion and an emitter etchback to create a selective emitter for p-type silicon solar cells [8-11]. In this work we apply this process for n-type silicon in order to create a selective front surface field.

6" reference and s-FSF solar cells with different FSF sheet resistances were processed, furthermore we investigate the influence of the Al paste and firing temperature on the emitter quality by QSSPC measurements. The etch-back and directly diffused FSF is characterized by measuring the emitter saturation current density  $j_{0E}$  vs. sheet resistance of symmetrical FZ-Si samples.

### 2 PROCESSING SEQUENCE

The processing sequence used to create the n-type solar cells with a selective FSF is based on the standard screen-printing process for p-type solar cells which is widely used in industrial production. For monocrystalline silicon, it starts with an alkaline random pyramid texture and a heavy  $\text{POCl}_3$  diffusion, the edge isolation is carried

out by single side etching. Subsequently the front surface is masked by inkjet or screen-printing in the area that will be contacted. The FSF is then etched back in an acidic solution to the desired sheet resistance. During the etching process, a thin layer of porous silicon is formed, which acts like an antireflective coating (ARC), so the sheet resistance and the etching homogeneity can be controlled by the wafer color. The porous silicon and the masking layer are subsequently removed in an alkaline solution. The following process steps remain unchanged from the standard p-type solar cell process, which continues with the plasma-enhanced chemical vapor deposition (PECVD) of  $\text{SiN}_x$ , screen-printing of the metallization and co-firing.

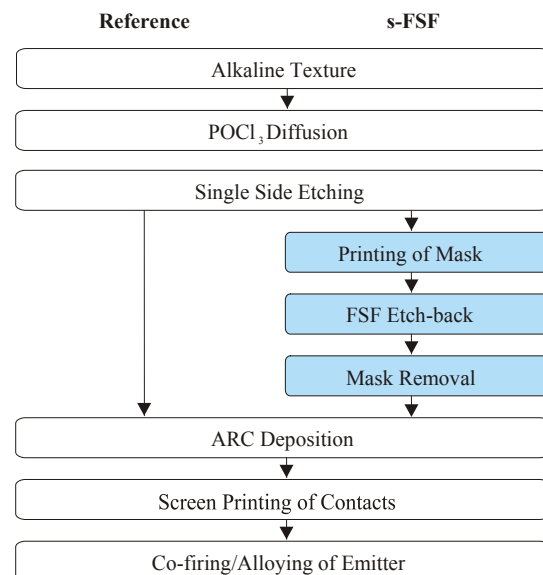


**Figure 1:** Processing sequence for the formation of a n-type solar cell with a selective FSF.

### 3 EXPERIMENTAL

#### 3.1. Emitter Characterization

In order to characterize the aluminum rear emitter quality, asymmetrical samples were fabricated from n-

type Cz silicon with a resistivity of 8  $\Omega\text{cm}$ . The samples were processed like a s-FSF cell solar without front side metallization (see Fig. 2) in order to obtain a comparable IR absorption. This allows directly transferring the firing temperature profile to the solar cell co-firing process.

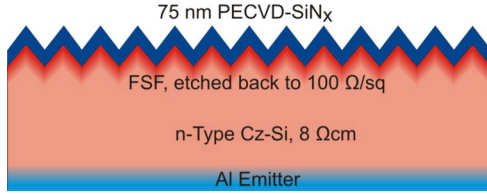


**Figure 2:** Structure of a QSSPC sample used to characterize the aluminum rear emitter quality.

After firing, the aluminum paste was removed in 37% HCl. The total saturation current density of the front FSF and the rear emitter was measured by QSSPC and evaluated in high level injection at a minority carrier density of  $1 \times 10^{16} \text{ cm}^{-3}$ . Although by knowing the FSF saturation current density the extraction of a  $j_{0E}$  from the rear emitter is possible in principal, this method leads to large errors due to the subtraction of the two values. Instead of this procedure an implied  $V_{OC}$  of the whole sample was calculated from the following expression, assuming a  $j_{SC}$  of  $38 \text{ mA/cm}^2$ :

$$V_{OC} = \frac{k_B T}{q} \left( \frac{j_{SC}}{j_{0E, total}} + 1 \right)$$

This voltage can be regarded as an upper limit for the cells'  $V_{OC}$  without losses contributed to the front side metallization and the low sheet resistance area below.

Fig. 3 shows the results of three different commercially available standard aluminum pastes versus the maximum firing temperature. The standard co-firing parameters for p-type cells were used.

For all pastes the  $V_{OC}$  increases with temperature to a maximum value. For the highest temperatures  $V_{OC}$  is reduced, on these samples strong inhomogeneities in the alloyed surface can be observed. When looking at the maximum  $V_{OC}$  values, paste C clearly outperforms pastes A and B.

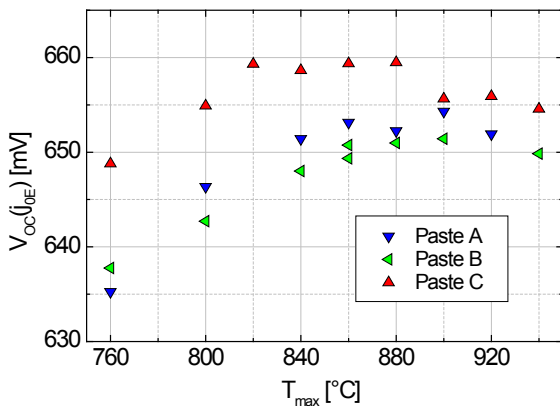


**Figure 3:** Implied  $V_{OC}$  vs. maximum firing temperature for three commercially available Al screen printing pastes.

### 3.2. FSF Characterization

In order to compare the directly diffused FSF to an etch-back FSF of the same sheet resistance, symmetrical QSSPC samples were processed from shiny etched 200  $\Omega\text{cm}$  p-type FZ silicon. The phosphorous diffusion then results in an emitter instead of a high-low junction, but this has no effect on the evaluation of the saturation current density.

Five  $\text{POCl}_3$  diffusions with target sheet resistances of 10, 30, 50, 80 and 110  $\Omega/\square$  were carried out only by changing the peak diffusion temperature. Etch-back emitter samples were etched from 10, 30, and 50  $\Omega/\square$  to various sheet resistances up to 110  $\Omega/\square$ . Before the  $\text{SiN}_x$  deposition, the sheet resistance was measured by a four point probe on both sides of each sample without the PSG. Finally, all samples were fired with standard solar cell co-firing parameters. The  $j_{0E}$  was evaluated at a minority carrier density of  $1 \times 10^{16} \text{ cm}^{-3}$ , the results are shown in Fig. 5.

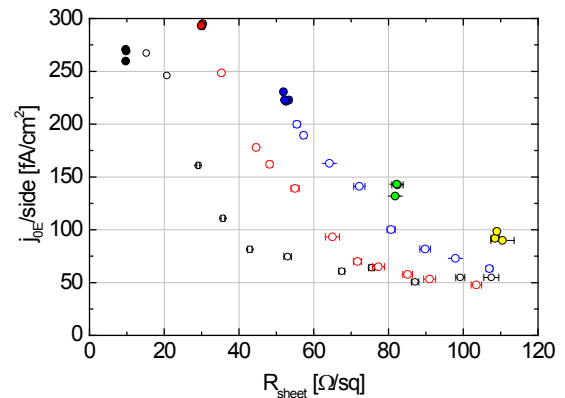


**Figure 5:**  $j_{0E}$  vs. sheet resistance of directly diffused samples (filled circles) and etched back samples (empty circles).

The directly diffused samples show a decay of  $j_{0E}$  with increasing  $R_{sheet}$  resulting in a best  $j_{0E}$  of  $90 \text{ fA/cm}^2$  for the 110  $\Omega/\square$  diffusion. On the etched back samples a strong reduction in  $j_{0E}$  compared to the directly diffused samples can be observed, the best results can be achieved when etching back from 10  $\Omega/\square$ . This behavior has already been investigated in [10] and can be explained by the deep doping profile with a lower phosphorous surface concentration of the etched back samples. Due to the different base resistivity, the absolute  $j_{0E}$  values in the work are not directly comparable to the ones published in [10].

When etching back from a very low sheet resistance, the etch-back depth necessary to obtain a sheet resistance of 60-100  $\Omega/\square$  strongly increases and therefore leads to a rounding of the valleys of the random pyramids [11].

The fact that the 10  $\Omega/\square$  samples feature a lower  $j_{0E}$  than the 30  $\Omega/\square$  samples has already been observed in previous experiments and might be caused by field effect passivation of the deep space charge region that passivates the surface even better than the PECVD- $\text{SiN}_x$  layer on a highly doped surface.

### 3.3. Solar Cell Results

We have processed five groups of 6 inch solar cells from 8  $\Omega\text{cm}$  n-type Cz silicon with a thickness of 175  $\mu\text{m}$  after texturization. A 50  $\Omega/\square$  FSF was chosen as a reference, the s-FSF cells were etched back from 35  $\Omega/\square$

to four different sheet resistances between 60 and 130  $\Omega/\square$ . The IV measurement results are shown in Fig. 6.

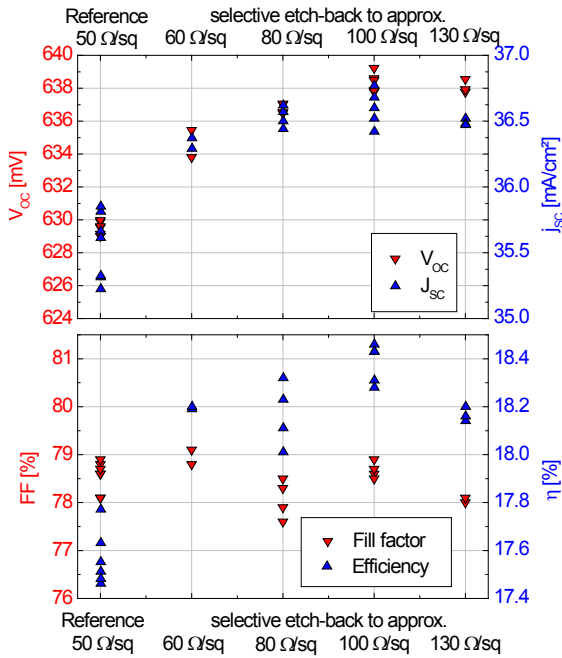


**Figure 6:** IV measurement results of the n-type reference and s-FSF solar cells with different etch-back depths.

The  $j_{SC}$  and  $V_{OC}$  of the s-FSF cells etched back to 100  $\Omega/\square$  show an average improvement of 1.1 mA/cm<sup>2</sup> and 9 mV respectively. For both values the differences between the groups etched back to 80 and 130  $\Omega/\square$  are small, which makes the process tolerant to sheet resistance inhomogeneities. The fill factor stays almost constant for all groups, which is due to the fact that the base contributes to the lateral conductivity, so the series resistance does not increase as much as for p-type selective emitter solar cells. A more detailed look at this effect can be found in [7]. The highest cell efficiency was 18.5% for a 100  $\Omega/\square$  s-FSF cell and an average gain of 0.8%<sub>abs</sub> of this group compared to the reference FSF cells was achieved.

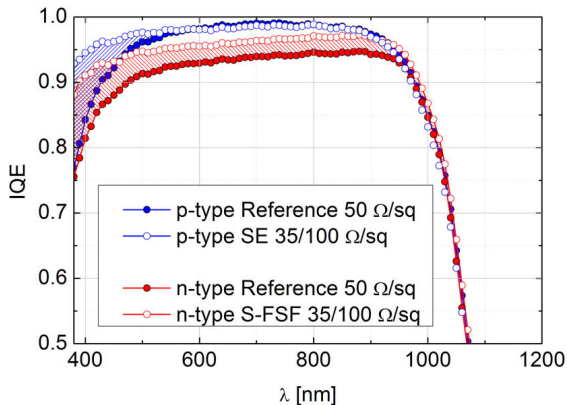


**Figure 7:** Comparison of the IQEs of a reference and a selectively doped solar cell from p- and n-type Cz silicon.

Fig. 7 shows the internal quantum efficiency (IQE) of reference and selectively etched (35/100  $\Omega/\square$ ) cells from

p- and n-type silicon. The values are scaled to the current measured on the cells by the IV measurement. The s-FSF cells show a clear improvement over a wide range of wavelengths, which can be confirmed by PC1D simulations. Since even for medium range wavelengths most of the charge carriers are generated close to the front surface but have to be collected by the rear emitter, the front surface passivation has a larger effect than for p-type solar cells. This explains the larger gain achieved by the selective front side doping on n-type compared to p-type silicon.

The solar cells were also evaluated by electroluminescence imaging, the best s-FSF cell is shown in Fig. 8. On all cells many finger interruptions behind the bus bars were caused by the snap-off behavior of the used screen. The pattern of the belt from the firing furnace is also visible which indicates inhomogeneities in the emitter quality caused by the firing process. This could possibly be avoided by an optimization of the firing parameters.

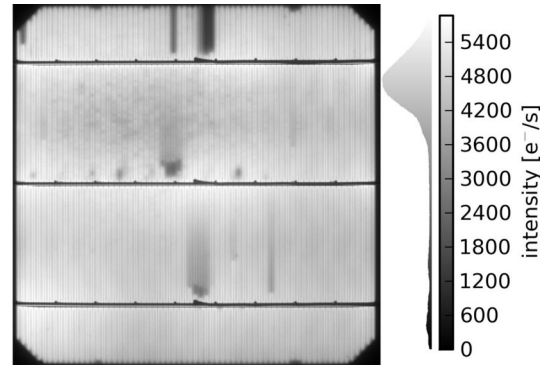


**Figure 8:** Electroluminescence image of the best s-FSF solar cell.

## 5 CONCLUSION

In this work we investigate the applicability of an etch-back process originally developed for formation of a selective emitter on p-type silicon solar cells. The process uses only one heavy diffusion, subsequently the emitter is masked by inkjet or screen printing and etched back in an acidic solution.

For n-type solar cells the process is unchanged, but the optimal choice of the etch-back sheet resistance is less limited by the series resistance contribution of the front diffusion, since the base has the same polarity and therefore improves the lateral conductivity.

We have tested three different aluminum pastes for the formation of the rear emitter by performing QSSPC measurements on asymmetrical samples that were fired at different temperatures.

The quality of different etch-back and directly diffused emitter samples was investigated by measuring  $j_{OE}$  under high level injection. When comparing the samples of same sheet resistance, the etch-back samples show a strong reduction in  $j_{OE}$  compared to a direct diffusion. The best values can be achieved by etching back from a very low sheet resistance, nevertheless the effect of an heavy etch-back on a surface texture has to be considered.

Large area solar cells were processed from n-type Cz silicon (8  $\Omega\text{cm}$ ), a reference FSF was compared to cells

with a selectively etched back FSF with four different sheet resistances between 60 and 130  $\Omega/\square$ . The best solar cell result of 18.5% was achieved etching back to 100  $\Omega/\square$ , the average gain of this group compared to the reference group is 0.8%<sub>abs</sub>. The IQE of the n-type s-FSF cells show an improvement over a wider wavelength range than of comparable p-type cells which leads to a higher gain in  $j_{SC}$ .

## 6 OUTLOOK

We have shown that the application of the etch-back selective emitter process to n-type silicon results in very high cell efficiencies and leads to a higher gain compared to p-type silicon. Further improvements could be achieved by applying a high refractive  $\text{SiN}_x$  stack [12] and by adapting the front electrode to the increased lateral conductivity. A more detailed optimization of the firing and printing parameters might also lead to increased cell efficiency.

In order to make the cell concept compatible to mass production, an interconnection technology without firing of AlAg soldering pads has to be developed. Possible solutions to this problem are proposed in [13, 14].

## 7 ACKNOWLEDGEMENTS

The financial support from the BMU project 0325079 is also gratefully acknowledged in particular for the processing and characterization equipment. The authors furthermore would like to thank B. Rettenmaier, L. Rothengaß-Mahlstaedt, F. Mutter, J. Ruck and S. Ohl for the processing support. The content of this publication is the responsibility of the authors.

## 8 REFERENCES

- [1] D. Macdonald et al.: 'Recombination activity of interstitial iron and other transition metal point defects in p- and n-type crystalline silicon', *Appl. Phys. Lett.* 85, 4061 (2004)
- [2] S. Glunz et al.: 'n-Type Silicon – Enabling Efficiencies > 20% in Industrial Production', *Proc. 35<sup>th</sup> IEEE PVSC, Honolulu, 2010*
- [3] D.L. Meier et al.: 'Aluminum Alloy Back p-n Junction Dendritic Web Silicon Solar Cell', *Solar Energy Materials and Solar Cells* 65, 2001, pp. 621-627
- [4] V.D. Mihailetschi et al.: '17.4% Efficiency Solar Cells on Large-Area and thin n-Type Silicon with Screen-Printed Aluminum-Alloyed Rear Emitter', *Proc. 22<sup>nd</sup> EPVSEC, Milan, 2007*
- [5] C. Schmiga et al.: 'Large-Area n-Type Silicon Solar Cells with Printed Contacts and Aluminum-Alloyed Rear Emitter', *Proc. 24<sup>th</sup> EPVSEC, Hamburg, 2009*
- [6] T. Schutz-Kuchly et al.: 'High Efficiency on Inversed Emitter n-Type Silicon Solar Cell Adapted to a Wide Range of Resistivity', *Proc. 24<sup>th</sup> EPVSEC, Hamburg, 2009*

- [7] K. Meyer et al.: 'All Screen-Printed Industrial n-Type Czochralski Silicon Solar Cells with Aluminium Rear Emitter and Selective FSF' *Proc. 35<sup>th</sup> IEEE PVSC, Honolulu, 2010*
- [8] H. Haverkamp et al.: 'Minimizing the Electrical Losses on the Front Side: Development of a Selective Emitter Process from a Single Diffusion', *Proc. 33<sup>rd</sup> IEEE PVSC, San Diego, 2008*
- [9] A. Dastgheib-Shirazi et al.: 'Selective Emitter for Industrial Solar Cell Production: a Wet Chemical Approach Using a Single Diffusion Process', *Proc. 23<sup>rd</sup> EU PVSEC, Valencia, 2008*, p. 1197
- [10] F. Book et al.: 'Detailed Analysis of High Sheet Resistance Emitters for Selectively Doped Silicon Solar Cells', *Proc. 24<sup>th</sup> EPVSEC, Hamburg, 2009*
- [11] F. Book et al.: 'The Etchback Selective Emitter Technology and its Application to Multicrystalline Silicon', *Proc. 35<sup>th</sup> IEEE PVSC, Hawaii, 2010*
- [12] A. Dastgheib-Shirazi et al.: 'Investigations of High Refractive Silicon Nitride Layers for Etched Back Emitters: Enhanced Surface Passivation for Selective Emitter Concept Cells – SECT', *Proc. 24<sup>th</sup> EU PVSEC, Hamburg, 2009*, p. 1600
- [13] A. Schneider et al.: 'The Day4<sup>TM</sup> Energy Electrode – A New Metallization Approach Towards Higher Solar Cell and Module Efficiency' *Proc. 21<sup>st</sup> EU PVSEC, Dresden, 2006*, p. 230
- [14] A. Halm et al.: 'Low Temperature Pads on Al-Emitter or Al-BSF' *Proc. 24<sup>th</sup> EU PVSEC, Hamburg, 2009*, p. 1462